Expression and distribution of Gpr119 in the pancreatic islets of mice and rats: Predominant localization in pancreatic polypeptide-secreting PP-cells ☆

Yukiko Sakamoto [a], Hiroshi Inoue [a,*], Shuhei Kawakami [a], Katsuyuki Miyawaki [a], Tatsuro Miyamoto [b], Kuniko Mizuta [c], Mitsuo Itakura [a]

[a] Institute for Genome Research, The University of Tokushima, Tokushima, Japan
[b] Department of Ophthalmology and Visual Neuroscience, The University of Tokushima, Tokushima, Japan
[c] Division of Cervico-Gnathostomatology, Hiroshima University Graduate School of Biomedical Sciences, Hiroshima, Japan

Abstract

The GPR119 was recently shown to be activated by oleoylethanolamide (OEA), a naturally occurring bioactive lipid with hypophagic and anti-obesity effects. In this study, we have cloned and characterized its murine counterpart, *Gpr119*. The full-length cDNA contained an open reading frame of 1008 bp encoding a 335-amino acid protein. The genomic organization of *Gpr119* was unique, having a 3′-untranslated second exon that was also involved in an alternative splicing event. Gene expression analyses confirmed its specific expressions in pancreatic islets and two endocrine cell-lines, MIN6 and αTC1. Immunohistochemistry and double-immunofluorescence studies using a specific antibody revealed the predominant Gpr119 localization in pancreatic polypeptide (PP)-cells of islets. No definitive evidence of Gpr119-immunoreactivity in adult β- or α-cells was obtained. The *Gpr119* mRNA levels were elevated in islets of obese hyperglycemic *db/db* mice as compared to control islets, suggesting a possible involvement of this receptor in the development of obesity and diabetes.
© 2006 Elsevier Inc. All rights reserved.

Keywords: Gpr119; Oleoylethanolamide; Pancreatic polypeptide

Bioactive lipid mediators such as lysophospholipids, eicosanoids, ether-lipids, endocannabinoids, and fatty-acids are playing important roles in the normal physiology of vascular, nervous and metabolic systems [1,2]. Among such lipids, the endogenous fatty-acid ethanolamide oleoylethanol amide (OEA) has attracted considerable attention because OEA is produced by cells in the small intestine in response to feeding and regulates satiety and body weight [3,4]. Recently, an orphan GPCR, GPR119, which is expressed predominantly in the human and rodent pancreas and gastrointestinal-tract and also in the rodent brain, has been shown to be activated by OEA [4]. Simultaneously, a selective small-molecule agonist of GPR119, PSN632408, was identified to suppress food intake in rats and, upon subchronic administration, to reduce body weight and adipose tissue deposition. These observations suggest that the

hypophagic effects of OEA are likely mediated via GPR119. On the other hand, lysophosphatidylcholine (LPC), another lipid mediator that has been described as enhancing insulin secretion from pancreatic islets, was independently reported to act as a GPR119 agonist [5]. GPR119 therefore represents a novel target for therapy aimed at obesity, diabetes, and related metabolic disorders.

At least two independent research groups reported similar but slightly different gene expression profiles of *GPR119* in other tissues as well as the pancreas [4,5]. In addition to the predominant expression in the pancreas, *GPR119* expressions have been demonstrated in isolated islets and murine insulinoma cell-lines, indicating specific expression in the β-cell lineage [5]. However, to date, there are no data corroborating its endogenous expression in any specific subtype of normal islet cells. As a first step toward complete characterization of the pattern of *GPR119* expression in the pancreas, in this study, we cloned and characterized the murine full-length *Gpr119* cDNA. We also developed a Gpr119-specific antibody that could be used for immunohistochemical study. Our results showed a predominant localization of Gpr119 in pancreatic polypeptide (PPY)-producing PP-cells, rather than in β-cells, within adult mouse and rat islets.

Materials and methods

Cell culture and animals. MIN6 and αTC1 were generously provided by Dr. Junichi Miyazaki (Osaka University) and Dr. Kazuyuki Hamaguchi (Oita University), respectively. All other cell-lines were obtained from the ATCC and maintained under standard cell-culture conditions. 10-week-old male BDF1 (Jcl:BDF1) mice, obese *db/db* (BKS.Cg-+Lepr^{db}/+Lepr^{db}/Jcl), and their lean control *m/m* (BKS.Cg-m+/m+/Jcl) littermates were purchased from CLEA (Tokyo, Japan). All animal experiments were conducted under approved IACUC protocols of the University of Tokushima.

RT-PCR, Northern blotting, and quantitative real-time RT-PCR. Mouse pancreatic islets were isolated using a standard collagenase digestion. Total RNA was purified using an RNeasy kit (Qiagen, Tokyo, Japan) including on-column DNase digestion. To completely eliminate contaminating DNA, RNA was retreated with DNase I (Takara, Shiga, Japan). For RT-PCR, primers for mouse *Gpr119* were designed based on the GenBank AY288423: mG119-F (5′-TGCAGCTGCCTCTGTCC TCA-3′) and mG119-R (5′-GCACAGGAGAGGGTCAGCAC-3′). A 100 ng of total RNA was reverse-transcribed to first-strand cDNA, and the PCR was performed under a standard amplification condition. The ORF of *Gpr119* was amplified using primers, CDS-F (5′-CAT GAGAATCTGAGCTCGCCATC-3′) and CDS-R (5′-TCCAGAGTGG GAAAGGGAAAGGCA-3′), with MIN6 cDNA and KOD-Plus DNA polymerase (Toyobo, Tokyo, Japan). A 1119 bp RT-PCR fragment was subcloned and sequenced using a Big-Dye Terminator kit v.3.1 (Applied Biosystems, Tokyo, Japan).

For Northern blotting, total RNA was separated on a 1% agarose–formalin gel and blotted onto a nylon-membrane. The membrane was probed with a *Gpr119* cDNA fragment, labeled with [α-^{32}P]dCTP (Amersham Biosciences, Piscataway, NJ, USA). Hybridization was performed overnight at 65 °C in modified Church–Gilbert buffer. After the stringency washes, the membrane was exposed to X-ray film.

The mRNA expressions of *Gpr119*, *Gpr40*, *Ins2* (*insulin II*), and *Ppy* were evaluated by TaqMan real-time RT-PCR method. Pre-developed assays were obtained from Applied Biosystems (*Gpr119*, Mm00731497_s1; *Gpr40*, Mm00809442_s1; *Ins2*, Mm00731595_gH; *Ppy*, Mm00435889_m1). RNAs from different mouse tissues were obtained from BD Biosciences

(Tokyo, Japan). Data were collected using the ABI 7900HT instrument and analyzed by a threshold cycle relative quantification method.

RLM-RACE. MIN6 cDNA was subjected to RLM (RNA ligase-mediated)-RACE using a GeneRacer kit (Invitrogen, Tokyo, Japan). For 5′-RACE, cDNA was subjected to two successive rounds of PCR using the following primers: mG119Race1 (5′-GCAAAGGCCAACACCATCATT CT-3′) and *nested* mG119Race2 (5′-CCAGAAATAGCCACGCCAATC AA-3′). The primers used for 3′-RACE were as follows: mG119Race3 (5′-TATTGGCAGAGGGAGGTTCGGCAG-3′) and *nested* mG119Race4 (5′-GAGAAAGCGCCTATCACATCGTCA-3′). The resulting 5′/3′-RACE products were gel-purified, subcloned, and analyzed by sequencing. To confirm the putative TSS determined by the 5′-RACE, RT-PCR was performed on MIN6 cDNA using either of sense primers, F1 or F2 (located upstream and downstream from TSS, respectively), and the common antisense primer R1: F1 (5′-GTAGAGGGGAGGGAC TAGCT-3′), F2 (5′-AGAGAGCTAGAAAAGCC GGA-3′) and R1 (5′-GGTAGCAGCACTTCCACTTA-3′).

Stable-expression of Gpr119-EGFP fusion construct and siRNA transfection. The full-length *Gpr119* cDNA with its C-terminal stop-codon replaced by one encoding alanine was generated by PCR, and inserted into the pEGFP-N1 (BD Biosciences). The recombinant pEGFP-Gpr119 plasmid was introduced into HEK293 cells using TransIT LT-1 (Mirus, Madison, WI, USA), and the stable transfectants were selected with 1.0 mg/ml geneticin (Promega, Madison, WI, USA). The EGFP expressions in living cells were visualized using an inverted Axiovert 200 microscope (Carl Zeiss, Tokyo, Japan). Two pre-designed siRNAs targeting *Gpr119* (Gpr119 siRNA1: #154760 and siRNA2: #154759) and the control Silencer-GFP siRNA were purchased from Ambion (Austin, TX, USA).

Measurement of cAMP production. OEA (*N*-oleoylethanolamine) and LPC (1-Oleoyl-*sn*-glycero-3-phosphocholine) were purchased from Sigma (St. Louis, MO, USA). HEK293 cells stably expressing either EGFP-Gpr119 fusion or control EGFP were plated on collagen-coated 96-well plates (Iwaki, Tokyo, Japan) at a density of 3×10^5 cells/well. After overnight incubation, the cells were preincubated with 0.5 mM IBMX (Sigma) at 37 °C for 30 min, followed by a 1-h incubation with test agents (10 μM OEA; 10 μM LPC; 10 μM forskolin [FSK]) or vehicle (0.4% ethanol plus 1% DMSO). The final concentration of FBS was 1% in all samples. The intracellular cAMP content was measured with a cAMP-EIA kit (Amersham). Transient-expression analysis of the wild-type *Gpr119* cDNA was conducted in COS-7 cells. Briefly, 10 μg of the pcDNA3.1-Gpr119 plasmid DNA was transfected at 1.5×10^6 cells/10-cm. The next day, transfected and mock cells were seeded in 24-well plates. Forty-eight hours after transfection, the cells were preincubated in BSA-free HBSS (pH 7.5) containing 0.5 mM IBMX at 37 °C for 30 min, and then treated for 1 h with test agents.

Antibody generation and immunoblotting. Based on the deduced mouse Gpr119 protein sequence, two peptides were synthesized: MG119 peptide-1 ([C]ARNRGPERTRESAY) and peptide-2 ([C]AGAYRPPRSVNDFK). Both peptides were conjugated to KLH through an additional N-terminal cysteine (C), and a mixture of these peptides was injected into Japanese white rabbits according to the proprietary immunization protocol (Japan Bio Services, Saitama, Japan). The mixture of synthetic peptides was also used simultaneously to affinity-purify the antibody.

Immunoblotting was performed according to standard protocols. Briefly, cells were harvested and the postnuclear fraction was pelleted by ultracentrifugation at 166,000*g* for 1 h. The resulting cellular-membrane fraction was resuspended, electrophoresed on a 10% SDS–PAGE gel, and transferred to a PVDF membrane. Membranes were incubated overnight at 4 °C with anti-Gpr119 antibody (1:500) diluted in PBS containing 5% nonfat dried milk. The immunoreactive bands were visualized using an ECL Plus detection kit (Amersham).

Immunohistochemistry and double immunofluorescence. BDF1 mice were anesthetized and transcardially perfused with 10% formalin. Pancreata were postfixed and embedded in paraffin blocks, and the 4 μm-thick sections were prepared. Additional rat sections were obtained from Genostaff (Tokyo, Japan). After deparaffination, the antigen retrieval was performed by heating the sections at 95 °C for 10 min in citrate buffer

(pH 6.0). Immunohistochemistry was perfomed using a Histomouse-Plus AEC kit (Zymed, South San Francisco, CA, USA). To detect Gpr119-immunoreactivity, sections were incubated at room temperature for 1 h with anti-Gpr119 antibody (1:500). Negative control staining was carried out with normal rabbit IgG (Sigma).

Double-immunofluorescence staining was performed as described previously [6], with some modifications. Sections were first incubated at room temperature for 1 h with one of the following: guinea pig anti-insulin antibody (1:200; Dako, Carpintera, CA, USA), rabbit anti-glucagon antibody (1:200), rabbit anti-somatostatin antibody (1:300) or rabbit anti-PPY antibody (1:500), followed by incubation with either Cy3-labeled goat anti-guinea pig or anti-rabbit IgG (1:500; Chemicon, Temecula, CA, USA). Sections were then heated in citrate buffer at 95 °C for 10 min and incubated overnight at 4 °C with anti-Gpr119 antibody (1:50), followed by incubation with FITC-labeled goat anti-rabbit IgG (1:200). The fluorescence images were acquired using an Axioplan-2 microscope (Carl Zeiss).

Results and discussion

Tissue- and cell-specific Gpr119 transcription

Consistent with a previous report [5], the presence of Gpr119 mRNA was clear both in islets and MIN6 cells (Fig. 1A). Northern analysis confirmed the expression in MIN6 and detected two Gpr119 transcripts: a major 2.3 kb and a minor 3.4 kb bands (Fig. 1B). No signal was observed in myoblast C2C12, whereas a faint smear band of ~2.3 kb was detectable in fibroblast NIH3T3 cells. This was presumably due to non-specific cross-hybridization, because repeated RT-PCR and sensitive real-time RT-PCR could not confirm Gpr119 expression in these cells.

Quantitative real-time RT-PCR analysis revealed both tissue- and cell-type-specific expressions of the Gpr119 (Fig. 1C left). Among various tissues and embryos at different stages, significant Gpr119 expression was found only in islets. We also tested four murine cell-lines and confirmed high Gpr119 expression in MIN6. Notably, Gpr119 transcription was also detectable in αTC1, a glucagonoma cell-line, and its expression was confirmed by RT-PCR followed by direct sequencing (data not shown). Overall, the Gpr119 expression pattern was similar to that of the β-cell specific GPCR, Gpr40 (Fig. 1C right; [7]), although there were some notable differences (e.g., MIN6/islet mRNA ratio).
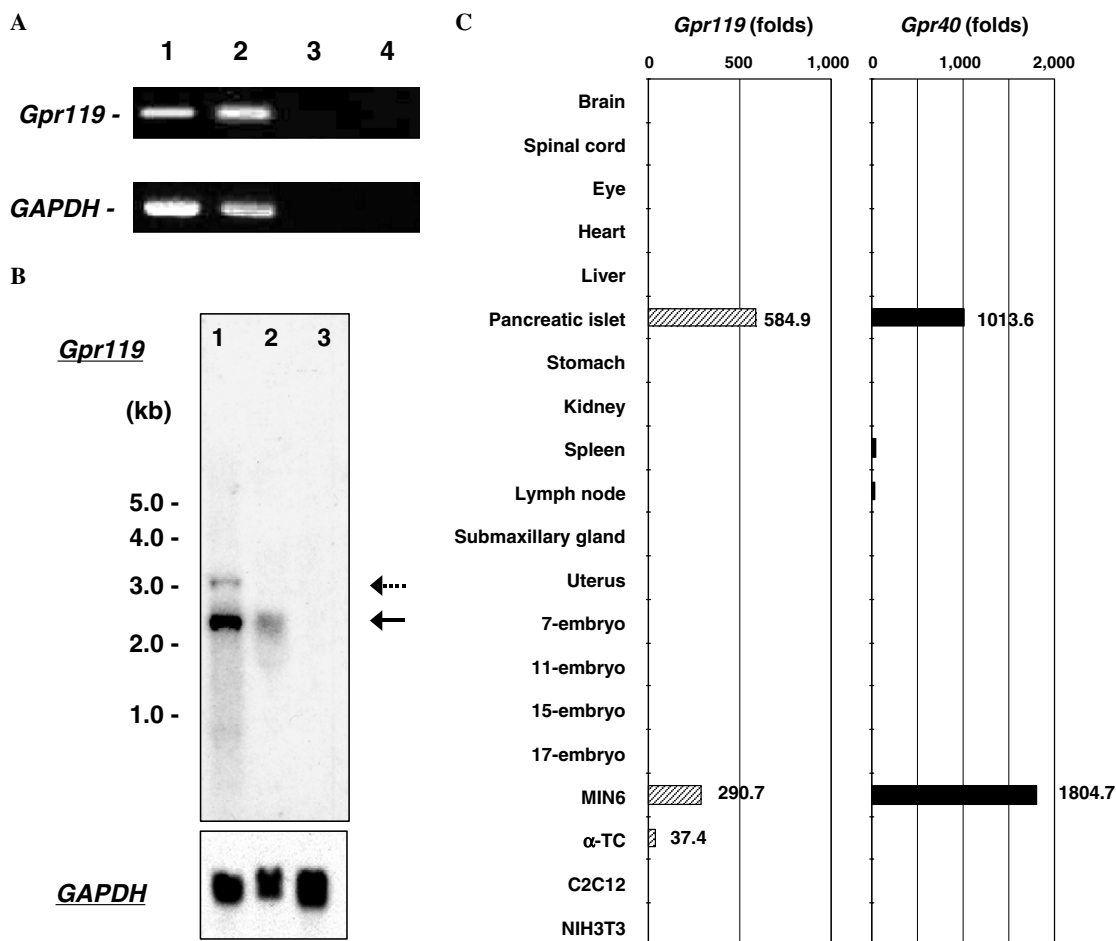

Fig. 1. Analysis of Gpr119 mRNA expression. (A) RT-PCR was performed for Gpr119 (upper; 252 bp) and GAPDH (lower; 109 bp). Lane 1, amplicon from mouse islet cDNA; lane 2, MIN6 cDNA; lane 3, minus-RT negative control; lane 4, no template control. (B) Northern blot was probed with either ^{32}P-labeled Gpr119 (upper) or GAPDH (lower) cDNA probes. Lane 1, MIN6; lane 2, NIH3T3; lane 3, C2C12. The black and dashed arrows indicate 2.3-kb (major) and 3.4-kb (minor) transcripts, respectively. (C) Relative mRNA levels in tissues and cell-lines (indicated on the right) are evaluated by TaqMan real-time RT-PCR (left, Gpr119; right, Gpr40). Data are presented as the average mRNA level after normalization to β-actin. The level for liver RNA was arbitrarily set at 1.0.

Characterization of full-length Gpr119 cDNA

To obtain full-length *Gpr119* cDNA, we conducted 5′/3′-RLM-RACE analysis using MIN6 cDNA. By 5′-RACE reaction, a single product of ~400 bp was identified (Fig. S1A; see supplemental materials). After subcloning of the amplicons, 17 subclones contained sequences homologous to *Gpr119*, of which 11 and 6 clones extended to 220 and 218 nt upstream from the initiator ATG codon, respectively, indicating that there are two close but separate major transcription start sites (TSS). These TSS were confirmed by RT-PCR using MIN6 cDNA and multiple primer combinations (Fig. S1B). The 3′-RACE generated a broad ladder band profile of ~1.0 kb, and the sequences of 36 subclones revealed the band of this nature to have two main causes. First, the differential usage of alternative polyadenylation sites produced transcripts of variable lengths in the 3′-end (data not shown). Second, we observed an alternative splicing event, lacking an internal 233 bp sequence in the 3′-UTR (11/36 subclones; Fig. S1C and S2).

Alignment of 5′- and 3′-RACE sequences resulted in the longest cDNA sequence of 2278 bp, with an ORF of 1008 bp (GenBank AB233291; Fig. S2). The deduced sequence predicted 335 amino-acid residues, with a characteristic seven-transmembrane helix topology of GPCR. We concluded the sequence to be full-length since it was consistent with the major transcript size in Northern analysis (2.3 kb), while the nature of the 3.4 kb minor transcript remains to be elucidated. Comparison of cDNA sequences with the mouse genomic sequences in the UCSC genome browser indicated the *Gpr119* gene to be encoded by two exons, separated by a 4231 bp intron. The entire ORF was contained within exon 1, and the differential splicing was implicated in an alternative splice acceptor site utilization at the 233 nt downstream from the first acceptor site. Previous bioinformatics analysis of the GPCR gene structure indicated more than 90% of GPCR genes to be intronless in their ORFs, and some to have intron(s) in their 5′-UTR [8]. To our knowledge, however, no examples have been found with intron(s) 3′ to the coding region. Thus, the murine *Gpr119* gene appears to exhibit a unique genomic structural feature distinguishing it from other GPCR genes.

Effects of overexpression of Gpr119-EGFP fusion

To analyze the subcellular distribution of Gpr119 protein, we prepared a *Gpr119* construct fused at the C-termini with EGFP and stably expressed it in HEK293. Three independent clones (119A, B, and C) were established and, in all clones, the fluorescence distribution was characteristic of a plasma-membrane labeling pattern (Fig. 2A upper). We next evaluated putative functionality of Gpr119-EGFP

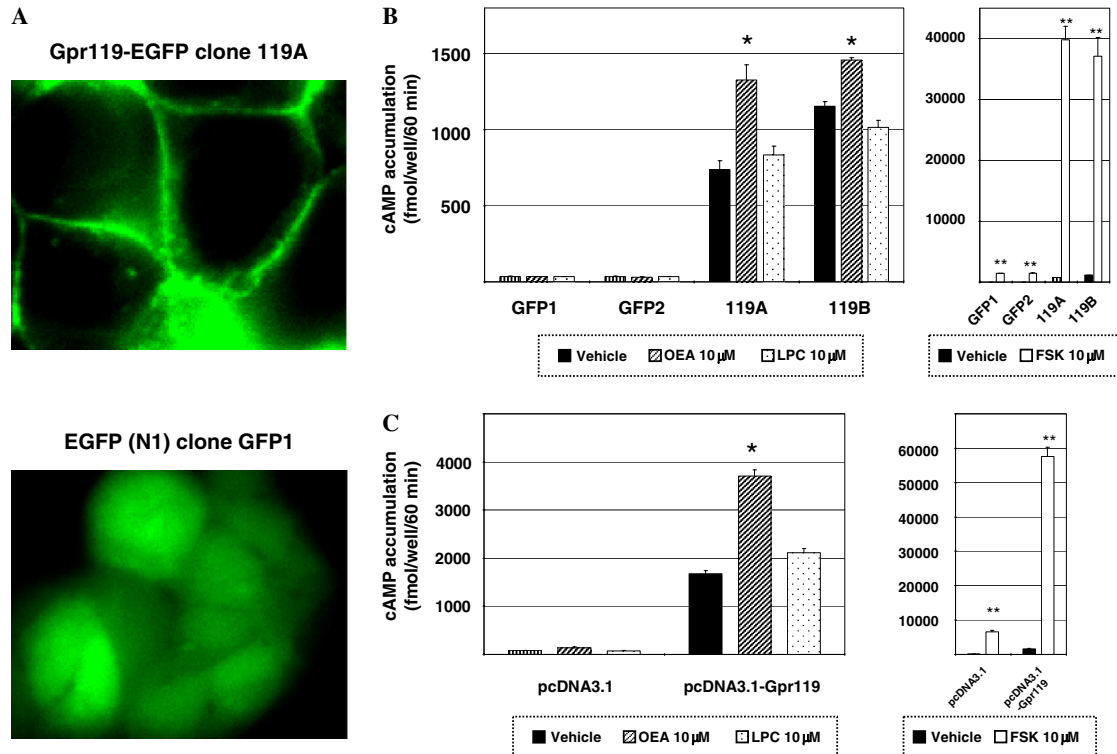Fig. 2. Stable expression of Gpr119-EGFP fusion protein in HEK293 cells. (A) A representative fluorescence image showing plasma-membrane localization of the Gpr119-EGFP fusion (upper; 119A). Control EGFP clone shows global fluorescence (lower; GFP1). (B) Intracellular cAMP levels were measured in Gpr119-EGFP (119A and B) and control EGFP (GFP1 and 2) clones. Cells were treated for 1 h with either vehicle (black), 10 μM OEA (hatched), 10 μM LPC (dotted) or 10 μM FSK (white), in the presence of 1% FBS. Data were expressed as means ± SEM of at least triplicate experiments. A 2-tailed unpaired *t* test was used for statistical testing. $^*P < 0.005$, $^{**}P < 0.0001$ versus respective basal. (C) COS-7 cells were transiently transfected with pcDNA3.1-Gpr119, and the cAMP contents were measured as described above, except without FBS. $^*P < 0.001$, $^{**}P < 0.0001$.

by measuring intracellular cAMP production. Basal cAMP levels in the Gpr119-EGFP clones were 20- to 30-fold higher than those in control clones (Fig. 2B left), indicating that the overexpression of Gpr119-EGFP leads to a constitutive activation of Gs subunit-mediated pathways. Interestingly, in these clones, FSK-stimulated cAMP production was also exaggerated (Fig. 2B right). Previous studies have demonstrated that either OEA or LPC can act as a GPR119 agonist and stimulate cAMP production, with a sub-maximum concentration of 10 μM [4,5]. In our experiment system, OEA stimulation of Gpr119-EGFP clones resulted in a significant increase in cAMP accumulations (Fig. 2B left; 1.79- and 1.26-fold increase in 119A and 119B, respectively), whereas LPC had no statistically significant effects. Neither OEA nor LPC had any effects on cAMP production in control EGFP clones.

One concern is that the experiments using HEK293 cells were conducted in the presence of reduced serum (1% FBS), since, without serum, both Gpr119-EGFP and control EGFP clones became non-adherent and detached from the culture dishes, resulting in variable assay results. For LPC, however, binding to serum albumin has been reported to be a critical determinant of pharmacokinetics [5]. We therefore performed additional experiments under serum-free conditions using COS-7 cells transiently transfected with Gpr119 cDNA; however, the results were essentially the same as those for the HEK293 clones, and LPC had no effect on the cAMP levels (Fig. 2C). Moreover, in both

Gpr119 and mock-transfected COS-7 cells, we observed cell-shape changes and rounding only with LPC treatment, indicating that LPC may be toxic to these cells (data not shown).

Characterization of anti-Gpr119 antibody

A rabbit polyclonal antibody specific for Gpr119 was generated. The specificity of antibody was tested in immunoblotting with lysates from Gpr119-EGFP clones. With a standard immunoblot protocol, in which cell lysates are boiled for 5 min prior to electrophoresis, the anti-Gpr119 antibody detected a high molecular weight mass of >300 kDa (Fig. S3A right). This was presumably due to protein aggregation, as is often seen in cases with other integral membrane proteins. In samples without heat-denaturing, the antibody recognized two distinct immunoreactive bands, a major 43 kDa and a minor 53 kDa bands. These were smaller than the predicted molecular weight of Gpr119-EGFP (∼65 kDa); however, we reasoned that the bands represent Gpr119-EGFP for the following reasons. First, the two bands were verified by use of an anti-EGFP antibody, although the intensity ratios of these bands were the exact opposite of the case with anti-Gpr119 antibody (Fig. S3A left). This might be because the antibodies recognize different epitopes with differences in conformational status. Second, the bands were specifically eliminated by either Gpr119 or EGFP siRNA transfection (Fig. S3B). We speculate that the aberrant migration pattern might
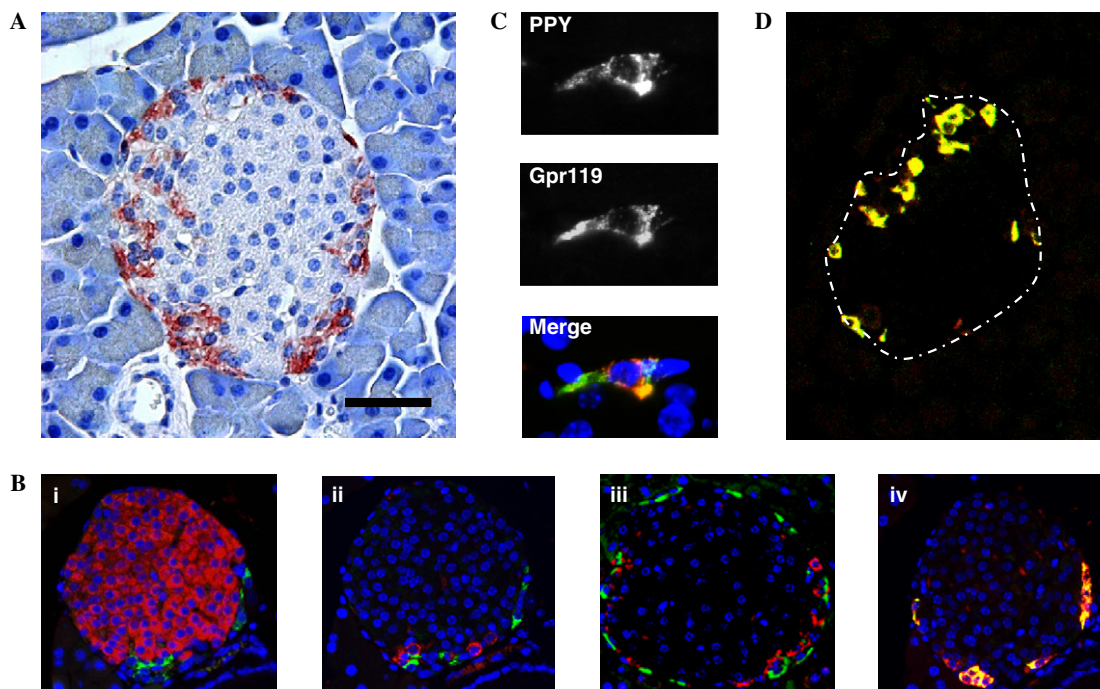

Fig. 3. Immunohistochemistry and double-immunofluorescence analysis of pancreatic islets. (A) A representative Gpr119-staining of adult mouse pancreatic islet (red; AEC chromogen). Bar = 50 μm. (B) Mouse islets were double-immunostained for Gpr119 (green; i–iv) and islet hormones (red; i, insulin; ii, glucagon; iii, somatostatin; iv, PPY). Note that the overlapping of red and green signals results in the appearance of yellow (iv). (C) Immunofluorescence signals for PPY (upper), Gpr119 (middle), and a merged image (lower). (D) Double-immunostained rat islet section (a merged image of Gpr119 and PPY). Dashed circle indicates location of the islet.

be due to unknown posttranslational modification(s). In addition, we tested whether anti-Gpr119 antibody could detect the endogenous Gpr119 in extracts of islets or MIN6, but failed presumably due to the low protein levels (data not shown).

Gpr119-immunohistochemistry in pancreatic islet

To identify the cellular distribution of Gpr119 protein in islets, an immunohistochemical staining of mouse pancreas was carried out with anti-Gpr119 antibody. Gpr119-immunoreactivity was clearly demonstrated in a subpopulation of endocrine cells located in the islet periphery (Fig. 3A). No signal was observed outside the islets, and the Gpr119-staining was abolished when the antibody was replaced with normal rabbit IgG (data not shown). Among individual islets, there was significant heterogeneity in the percentage of islet cells immunopositive for Gpr119, ranging from 0 to 9%. The Gpr119-immunopositive cells were most abundant in islets located in the duodenal lobe of pancreas (data not shown).

To determine the islet cell-type responsible for Gpr119-immunoreactivity, double-immunofluorescence studies were performed. As shown in Fig. 3B (iv), the signals for Gpr119 largely overlapped with PPY signals. At the single-cell level, Gpr119-immunofluorescence was observed in more peripheral regions of cells, while PPY showed cytoplasmic staining with prominent perinuclear accentuation (Fig. 3C). Similar results were obtained in rat pancreas sections (Fig. 3D). Previous studies have identified PP-cells as expressing several non-tissue-specific GPCRs such as

somatostatin receptor subtypes 1–5 [9]. To our knowledge, Gpr119 is the first GPCR whose intra-islet expression was proven to be PP-cell specific.

We obtained no definitive evidence of Gpr119-immunoreactivity in adult β- or α-cells. These observations may not necessarily correlate with mRNA expression data. We speculate that the Gpr119 mRNA expressions in MIN6 or αTC1 cell-lines may not reflect the cell-type specific gene expression pattern, but rather represents a shared feature of endocrine precursor cells.

Gpr119 expression in db/db islets

To explore the possible role of Gpr119 in the pathogenesis of obesity and diabetes, we examined islet Gpr119 mRNA expression in db/db mice, an obesity-induced type 2 diabetes model. In db/db mice, failure of β-cells to compensate for insulin resistance is thought to be responsible for the development of diabetes, and, in islets, it has been reported that the expressions of β-cell genes important for glucose sensing and insulin secretion are decreased (e.g., GLUT2 and Kir6.2), whereas genes involved in insulin biosynthesis are essentially preserved [10]. At 10 weeks of age, we confirmed that db/db mice were significantly obese and hyperglycemic (Fig. S4). Consistent with previous reports, our real-time RT-PCR showed that the Ins2 mRNA levels in db/db islets were not significantly changed as compared to control m/m islets, although they did tend to be lower (Fig. 4). Gpr40 mRNA was significantly decreased to 36.8%, confirming involvement of the gene in glucose sensing and insulin secretion. Interestingly,
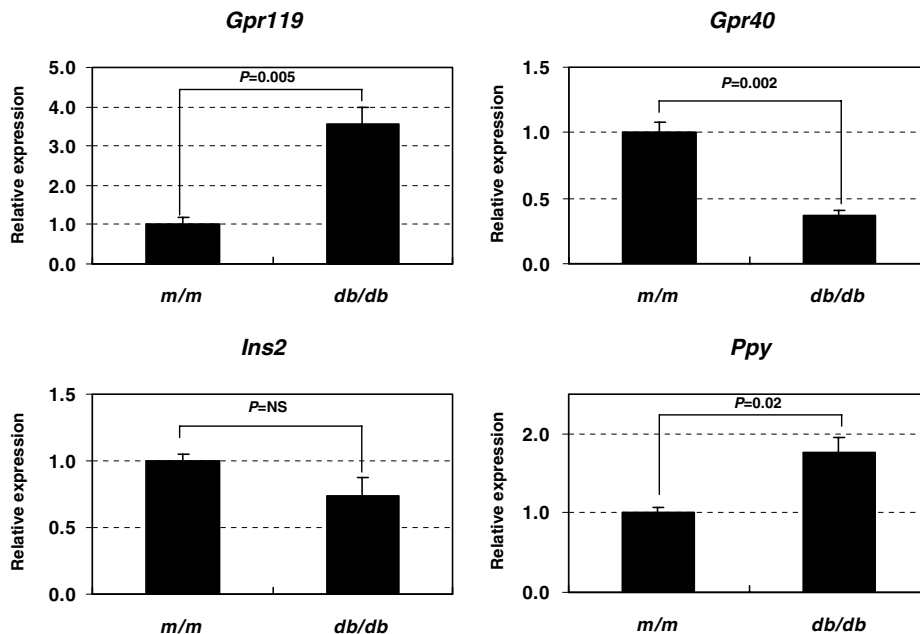

Fig. 4. Quantitative analysis of Gpr119 expression in islets of db/db mice. The quantitative expression levels of Gpr119, Gpr40, Ins2, and Ppy were measured in 10-week db/db ($n = 3$) and control m/m ($n = 3$) islets. After normalization to β-actin, the mRNA level for each gene in control islets was arbitrarily set at 1.0. Data were expressed as means ± SEM. A 2-tailed unpaired t-test was used for statistical testing.

Gpr119 expression was markedly increased to 356.9% in _db/db_ islets. The _Ppy_ mRNA showed expression changes in the same direction as that of _Gpr119_, and were significantly increased. These changes in mRNA expressions could be due to an increased PP-cell volume density per islet; however, in immunohistochemistry, there was no obvious alteration in the relative proportion of either Gpr119- or PPY-immunopositive cells in 10-week _db/db_ islets (data not shown).

Conclusion and implications

Islet PP-cells secrete PPY. PPY exerts a variety of regulatory actions, including inhibition of pancreatic exocrine secretion, gallbladder contraction, and modulation of gastrointestinal motility [11]. These effects together slow down the digestive process and the entry of nutrients into the circulation, preventing the postprandial elevation of blood glucose. Interestingly, altered PPY secretion has been described in patients with clinical syndromes associated with abnormal eating behaviors [12]: a decreased postprandial secretion of PPY has been described in patients with Prader–Willi syndrome, a genetic form of obesity, whereas an exaggerated secretion was observed in subjects with anorexia nervosa. In view of our experimental results showing Gpr119 to predominantly be localized in islet PP-cells and the altered mRNA expressions in islets of obese diabetic _db/db_ mice, it is tempting to speculate that intestinally produced OEA may reach islets and stimulate PPY secretion, and that the hypophagic effects of OEA are mediated, at least in part, through PPY. Further elucidation of the actual physiological and pharmacological relevance of Gpr119-signaling in PP-cells might open the way to new strategies for obesity and type 2 diabetes management.

Acknowledgments

Appendix A. Supplementary data

Supplementary data associated with this article can be found, in the online version, at doi:10.1016/j.bbrc.2006.10.076.

References

[1] D.S. Im, Discovery of new G protein-coupled receptors for lipid mediators, J. Lipid Res. 45 (2004) 410–418.

[2] T. Hla, Genomic insights into mediator lipidomics, Prostaglandins Other Lipid Mediat. 77 (2005) 197–209.

[3] J. Lo Verme, S. Gaetani, J. Fu, F. Oveisi, K. Burton, D. Piomelli, Regulation of food intake by oleoylethanolamide, Cell. Mol. Life Sci. 62 (2005) 708–716.

[4] H.A. Overton, A.J. Babbs, S.M. Doel, M.C. Fyfe, L.S. Gardner, G. Griffin, H.C. Jackson, M.J. Procter, C.M. Rasamison, M. Tang-Christensen, P.S. Widdowson, G.M. Williams, C. Reynet, Deorphanization of a G protein-coupled receptor for oleoylethanolamide and its use in the discovery of small-molecule hypophagic agents, Cell Metab. 3 (2006) 167–175.

[5] T. Soga, T. Ohishi, T. Matsui, T. Saito, M. Matsumoto, J. Takasaki, S. Matsumoto, M. Kamohara, H. Hiyama, S. Yoshida, K. Momose, Y. Ueda, H. Matsushime, M. Kobori, K. Furuichi, Lysophosphatidylcholine enhances glucose-dependent insulin secretion via an orphan G-protein-coupled receptor, Biochem. Biophys. Res. Commun. 326 (2005) 744–751.

[6] D. Tornehave, D.M. Hougaard, L. Larsson, Microwaving for double indirect immunofluorescence with primary antibodies from the same species and for staining of mouse tissues with mouse monoclonal antibodies, Histochem. Cell Biol. 113 (2000) 19–23.

[7] Y. Itoh, Y. Kawamata, M. Harada, M. Kobayashi, R. Fujii, S. Fukusumi, K. Ogi, M. Hosoya, Y. Tanaka, H. Uejima, H. Tanaka, M. Maruyama, R. Satoh, S. Okubo, H. Kizawa, H. Komatsu, F. Matsumura, Y. Noguchi, T. Shinohara, S. Hinuma, Y. Fujisawa, M. Fujino, Free fatty acids regulate insulin secretion from pancreatic beta cells through GPR40, Nature 422 (2003) 173–176.

[8] A.J. Gentles, S. Karlin, Why are human G-protein-coupled receptors predominantly intronless? Trends Genet. 15 (1999) 47–49.

[9] E. Ludvigsen, R. Olsson, M. Stridsberg, E.T. Janson, S. Sandler, Expression and distribution of somatostatin receptor subtypes in the pancreatic islets of mice and rats, J. Histochem. Cytochem. 52 (2004) 391–400.

[10] C. Kjorholt, M.C. Akerfeldt, T.J. Biden, D.R. Laybutt, Chronic hyperglycemia, independent of plasma lipid levels, is sufficient for the loss of beta-cell differentiation and secretory function in the db/db mouse model of diabetes, Diabetes 54 (2005) 2755–2763.

[11] G. Katsuura, A. Asakawa, A. Inui, Roles of pancreatic polypeptide in regulation of food intake, Peptides 23 (2002) 323–329.

[12] K. Wynne, S. Stanley, B. McGowan, S. Bloom, Appetite control, J. Endocrinol. 184 (2005) 291–318.